Excess Enthalpies and Volumes for Mixtures of Chlorobenzene with Some Aromatic Hydrocarbons at 298.15 K

Reiji Tanaka[†] and George C. Benson*

Division of Chemistry, National Research Council of Canada, Ottawa, Ontario, Canada K1A 0R6

Measurements of excess enthalpies in a flow microcalorimeter and of excess volumes in a successive dilution dilatometer were carried out at 298.15 K for binary mixtures of chlorobenzene with benzene, toluene, ethylbenzene, o-xylene, m-xylene, and p-xylene.

The purpose of this paper is to report measurements of excess enthalpies and volumes for binary mixtures of chlorobenzene with benzene, toluene, ethylbenzene, and the three isomeric xylenes. At present there are several different views regarding the attractive interaction between unlike molecules in halobenzene–aromatic hydrocarbon mixtures (*3, 5, 13, 14, 16*). Accumulation of further information about the thermodynamic properties of such mixtures is essential to a more complete understanding of the nature of the interaction.

[†] Presently at the Department of Chemistry, Faculty of Science, Osaka City University, Sumiyoshi-ku, Osaka, Japan.

Table I. Physical Properties of Component Liquids at 298.15 K

| | Density, g cm^{-3} | | n_D | |
	Measd	Lit.	Measd	Lit.
Benzene	0.87364	0.87368 (*1*)	1.49794	1.49792 (*1*)
Toluene	0.86224	0.86228 (*1*)	1.49410	1.49414 (*1*)
Ethylbenz-ene	0.86261	0.86262 (*1*)	1.49315	1.49320 (*1*)
o-Xylene	0.87582	0.87594 (*1*)	1.50260	1.50295 (*1*)
m-Xylene	0.85980	0.85988 (*1*)	1.49467	1.49464 (*1*)
p-Xylene	0.85669	0.85667 (*1*)	1.49318	1.49325 (*1*)
Chloro-benzene	1.10110	1.10090 (*17*)	1.52176	1.52211 (*17*)

Experimental Section

Excess enthalpies were determined in an LKB flow microcalorimeter. Details of the auxiliary equipment and of the operating procedure have been described previously (*18*). The magnitude of the total error in the determination of H^E is less than $(0.1 + 0.005| H^E|)$ J mol^{-1}.

Excess volumes were measured at constant pressure by a successive dilution technique using a micrometer syringe dilatometer which has also been described previously (*19*). For the present systems the error in the measurement of the excess volume is estimated to be less than $(0.0003 + 0.003| V^E|)$ cm^3 mol^{-1}.

The component liquids were purified chromatographically. Densities and refractive indices at 298.15 K, characterizing the samples used for the measurements, are listed in Table I along with values from the literature (*1, 17*) for comparison.

Results and Discussion

Experimental values of the excess enthalpies and volumes determined at 298.15 K are listed in Tables II and III, respectively, and are also presented graphically in Figures 1–6. Different symbols are used to indicate the results for V^E obtained in two separate dilution runs on each system. In all cases x_1 is the mole fraction of chlorobenzene.

Each set of results was fitted with a smoothing function of the form

$$X^E = x_1 x_2 \sum_1^n c_j (x_2 - x_1)^{j-1} \tag{1}$$

where X^E represents either H^E or V^E. Values of the coefficients c_j were calculated by the method of least squares with equal weights assigned to all results. The minimum number (n) of

Table II. Molar Excess Enthalpies of Chlorobenzene (1)–Aromatic Hydrocarbon (2) Mixtures at 298.15 K

| | Component 2 (H^E, J mol^{-1}) | | | | | |
x_1	C_6H_6	$C_6H_5CH_3$	$C_6H_5C_2H_5$	o-$C_6H_4(CH_3)_2$	m-$C_6H_4(CH_3)_2$	p-$C_6H_4(CH_3)_2$
0.0500	—	−23.55	−29.57	−19.65	—	−22.18
0.1000	−2.00	−44.54	−55.22	−37.53	−39.71	−42.04
0.1500	−2.91	−63.18	−78.03	−53.54	−56.44	−60.22
0.2000	−3.69	−78.93	−98.02	−67.70	−70.88	−75.66
0.2500	−4.36	−91.98	−115.33	−79.60	−82.99	−88.77
0.3000	−4.89	−102.66	−129.30	−89.53	−93.19	−99.44
0.3500	−5.29	−110.04	−140.04	−97.55	−100.87	−107.75
0.4000	−5.53	−115.62	−147.76	−103.30	−106.26	−113.70
0.4500	−5.65	−118.36	−152.16	−106.77	−109.30	−117.23
0.5000	−5.65	−118.67	−153.20	−108.18	−110.08	−118.18
0.5000	−5.58	−118.60	−153.45	−108.13	−109.89	−118.36
0.5500	−5.53	−116.70	−151.71	−107.32	−108.53	−116.84
0.6000	−5.32	−112.55	−146.87	−104.27	−104.94	−112.75
0.6500	−4.97	−105.83	−139.03	−98.86	−98.90	−106.40
0.7000	−4.50	−96.89	−127.77	−91.31	−90.91	−97.67
0.7500	−3.95	−85.88	−113.94	−81.57	−80.57	−86.78
0.8000	−3.33	−72.72	−96.33	−69.39	−68.33	−73.61
0.8500	−2.57	−57.35	−76.83	−55.55	−54.10	−58.09
0.9000	−1.86	−39.93	−54.13	−38.97	−37.89	−40.67
0.9500	—	−21.08	−28.39	−20.50	−19.84	−21.21

Table III. Molar Excess Volumes of Chlorobenzene (1)–Aromatic Hydrocarbon (2) Mixtures at 298.15 K

x_1	V^E, cm^3 mol^{-1}	x_1	V^E, cm^3 mol^{-1}	x_1	V^E, cm^3 mol^{-1}	x_1	V^E, cm^3 mol^{-1}
			Chlorobenzene (1)–Benzene (2)				
0.0462	0.0045	0.3690	0.0244	0.4909	0.0261	0.8198	0.0154
0.1001	0.0097	0.4124	0.0255	0.5306	0.0260	0.8698	0.0118
0.1433	0.0131	0.4270	0.0256	0.5774	0.0254	0.9175	0.0080
0.1861	0.0163	0.4511	0.0257	0.6339	0.0241	0.9666	0.0032
0.2564	0.0205	0.4561	0.0258	0.7029	0.0216		
0.3171	0.0229	0.4855	0.0258	0.7684	0.0185		
			Chlorobenzene (1)–Toluene (2)				
0.0564	−0.0207	0.3538	−0.0850	0.5169	−0.0896	0.7264	−0.0676
0.1157	−0.0393	0.4100	−0.0888	0.5320	−0.0891	0.7899	−0.0555
0.1667	−0.0535	0.4571	−0.0900	0.5560	−0.0876	0.8427	−0.0438
0.2191	−0.0651	0.4817	−0.0904	0.6034	−0.0841	0.8870	−0.0327
0.2872	−0.0772	0.4977	−0.0900	0.6609	−0.0774	0.9501	−0.0154
			Chlorobenzene (1)–Ethylbenzene (2)				
0.0578	−0.0291	0.3876	−0.1266	0.5944	−0.1250	0.8989	−0.0453
0.1329	−0.0622	0.4452	−0.1309	0.6414	−0.1188	0.9542	−0.0216
0.1867	−0.0820	0.4936	−0.1319	0.6937	−0.1090		
0.2439	−0.0991	0.5335	−0.1309	0.7569	−0.0936		
0.3174	−0.1160	0.5676	−0.1286	0.8340	−0.0699		
			Chlorobenzene (1)–o-Xylene (2)				
0.0535	−0.0054	0.3592	−0.0222	0.5499	−0.0237	0.7645	−0.0160
0.1238	−0.0106	0.4206	−0.0237	0.5539	−0.0233	0.8246	−0.0125
0.1772	−0.0142	0.4709	−0.0241	0.5952	−0.0228	0.8673	−0.0099
0.2306	−0.0167	0.5135	−0.0240	0.6444	−0.0213	0.9128	−0.0066
0.2997	−0.0201	0.5185	−0.0237	0.6999	−0.0194	0.9591	−0.0034
			Chlorobenzene (1)–m-Xylene (2)				
0.0571	−0.0114	0.3773	−0.0475	0.5658	−0.0476	0.8263	−0.0248
0.1230	−0.0227	0.4384	−0.0488	0.6014	−0.0462	0.8715	−0.0195
0.1783	−0.0304	0.4891	−0.0492	0.6490	−0.0432	0.9179	−0.0127
0.2376	−0.0374	0.5255	−0.0492	0.7042	−0.0385	0.9659	−0.0056
0.3012	−0.0433	0.5306	−0.0486	0.7685	−0.0319		
			Chlorobenzene (1)–p-Xylene (2)				
0.0475	−0.0143	0.3294	−0.0664	0.5728	−0.0716	0.8194	−0.0411
0.0934	−0.0265	0.3969	−0.0716	0.5971	−0.0706	0.8672	−0.0316
0.1449	−0.0384	0.4526	−0.0737	0.6421	−0.0664	0.9073	−0.0230
0.1958	−0.0480	0.4996	−0.0739	0.6969	−0.0609	0.9566	−0.0115
0.2546	−0.0578	0.5386	−0.0730	0.7621	−0.0510		

coefficients needed for an adequate representation of a set of m results was determined by examining the variation of the standard error

$$\sigma = [\sum_1{}^m\{X^E(\text{obsd}) - X^E(\text{equation 1})\}^2/(m - n)]^{1/2} \quad (2)$$

for increasing values of n. The coefficients and standard errors for the representations selected in this way are summarized in Table IV.

The solid curves in Figures 1–6 were calculated from eq 1, using the values of the coefficients from Table IV. Results taken from the literature are also plotted in these figures for comparison.

Chlorobenzene–benzene mixtures have been studied a number of times in the past (3–5, 7, 9, 12, 15, 20). In Figure 1, the results for H^E reported recently by Harsted and Thomsen (7) and by Tanaka et al. (20) agree reasonably with our findings, as does the extrapolation of the results of Nigam et al. (15), but Canning and Cheesman's (4) values at 297.48 K fall 1–2 J mol^{-1} below our curve. Within their estimated error, Harris and Dunlop's (6) values for V^E (see Figure 2) agree with our results, but the smoothed representation of V^E given by Letcher and Bayles (9) differs markedly.

The excess enthalpies for chlorobenzene–toluene determined at 297.48 K by Canning and Cheesman (4) lie 10–15 J mol^{-1}

above our curve in Figure 3. However, the equimolar value from the work of Becker et al. (2) and the dotted curve interpolated from the smoothing functions given by Harsted and Thomsen (7) are nearer to our results. The single value of H^E reported (16) for chlorobenzene–ethylbenzene does not differ significantly from our curve.

In Figure 4, Recko and Sadowska's (16) values for equimolar mixtures of chlorobenzene with toluene and with ethylbenzene agree reasonably with our results. The value for chlorobenzene–toluene extrapolated from the measurements of Nigam and Singh (12) appears to be low, but its estimation involved a rather large uncertainty.

The excess enthalpies of mixtures of chlorobenzene with the isomeric xylenes have not been studied previously at 298.15 K. However, the measurements for p-xylene at 293.15 K by Harsted and Thomsen (7) fall close to our curve (see Figure 5).

The excess volumes of chlorobenzene–isomeric xylene mixtures are plotted in Figure 6. The measurements by Nigam et al. (11) agree with our results but show more scatter.

In accord with the view that an attractive interaction exists between unlike molecules in halobenzene–aromatic hydrocarbon mixtures, the excess enthalpies for all of the present systems are negative. Their magnitude suggests that this interaction is smallest in chlorobenzene–benzene mixtures and that it increases significantly when benzene is replaced by one of
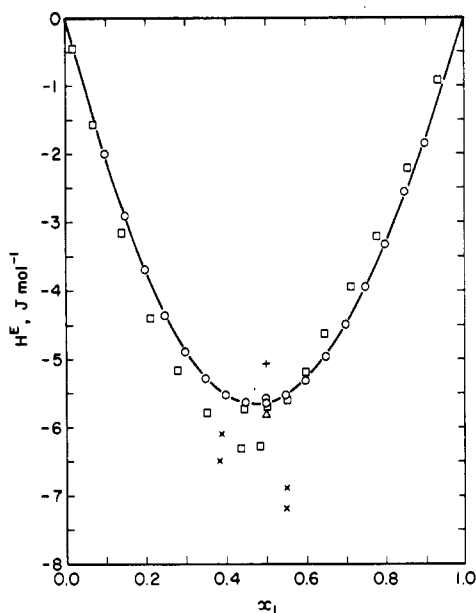
Figure 1. Molar excess enthalpy of chlorobenzene (1)–benzene (2) at 298.15 K: O, present work; □, Tanaka et al. (20); ×, Canning and Cheesman (4) at 297.48 K; +, interpolated from Harsted and Thomsen (7); △, extrapolated from Nigam et al. (15). Solid curve is least-squares representation of our results by eq 1.
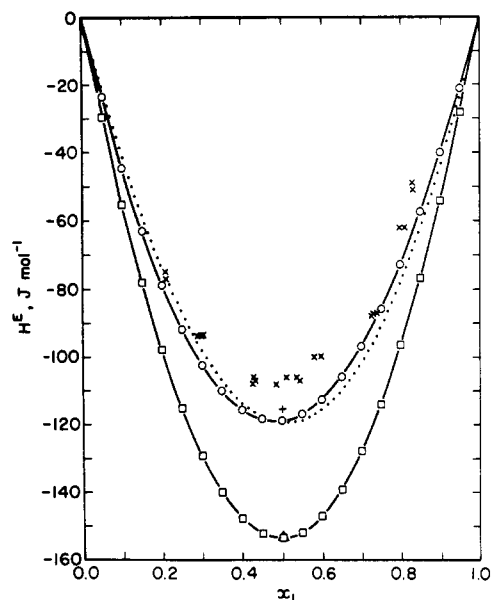

Figure 3. Molar excess enthalpies at 298.15 K. Chlorobenzene (1)–toluene (2): O, present work; ×, Canning and Cheesman (4) at 297.48 K; +, Becker et al. (2). Dotted curve interpolated from smoothing functions given by Harsted and Thomsen (7). Chlorobenzene (1)–ethylbenzene (2): □, present work; △, Recko and Sadowska (16). Solid curves are least-squares representations of our results by eq 1.
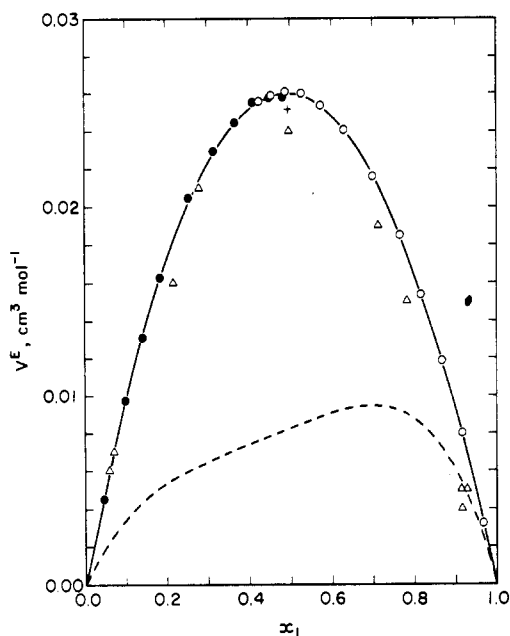

Figure 2. Molar excess volume of chlorobenzene (1)–benzene (2) at 298.15 K: O and ●, present work (two separate dilutions); △, Harris and Dunlop (6); +, extrapolated from Nigam and Singh (12). Broken curve was calculated from smoothing function given by Letcher and Bayles (9). Solid curve is least-squares representation of our results by eq 1.
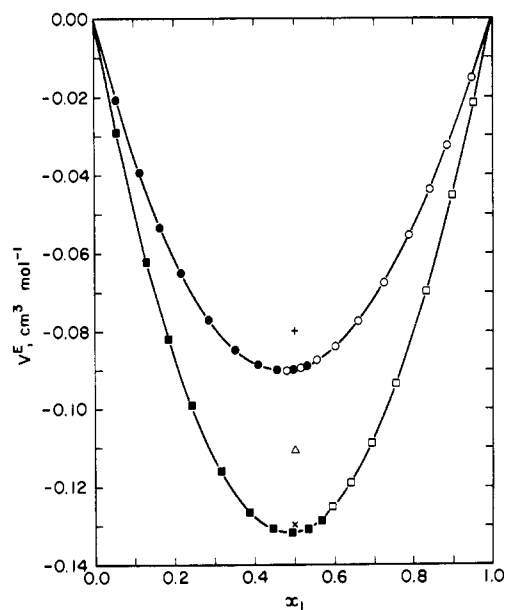

Figure 4. Molar excess volumes at 298.15 K. Chlorobenzene (1)–toluene (2): O and ●, present work (two separate dilutions); △, extrapolated from Nigam and Singh (12); +, Recko and Sadowska (16). Chlorobenzene (1)–ethylbenzene (2): □ and ■, present work (two separate dilutions); ×, Recko and Sadowska (16). Solid curves are least-squares representations of our results by eq 1.

the alkylbenzenes. It is interesting that the behavior of the excess volumes is qualitatively similar to that of the excess enthalpies, with the value of V^E decreasing between the benzene and the alkylbenzene mixtures. However, V^E is positive for the chlorobenzene–benzene system and negative for the others, possibly due to the difference in the relative sizes of the molecules.

Finally, we believe that the excess enthalpy of one of the systems that we have studied, chlorobenzene–toluene, merits further investigation with a view to establishing it as an exo-

thermic test system for mixing calorimeters. At present, only the endothermic mixing of cyclohexane with n-hexane has been officially recognized as a standard (8) and there is a need for a standard exothermic mixture. In the past, p-dioxane–carbon tetrachloride, benzene–dichloromethane, and dichloromethane–p-dioxane have been used in our laboratory in examining the performance of new calorimeters (10, 18). However, chlorobenzene–toluene is better suited for this purpose since the components are more stable and easier to purify.

Table IV. Coefficients and Standard Errors for Representation of Excess Functions of Chlorobenzene (1)–Aromatic Hydrocarbon (2) Mixtures by Equation 1

Component 2	Function[a]	c_1	c_2	c_3	c_4	σ
Benzene	H^E	−22.612	−2.599	1.899	1.977	0.03
	V^E	0.104 19	0.002 58	0.003 28		0.000 13
Toluene	H^E	−475.164	−32.411	5.227		0.16
	V^E	−0.360 05	−0.042 70	0.006 05	0.007 25	0.000 13
Ethylbenzene	H^E	−613.881	−8.190	11.982		0.22
	V^E	−0.526 94	−0.031 57	0.013 24	0.011 06	0.000 23
o-Xylene	H^E	−432.669	10.138	11.446		0.08
	V^E	−0.095 74	−0.006 82	0.008 83		0.000 25
m-Xylene	H^E	−440.241	−13.303	14.172		0.08
	V^E	−0.197 14	−0.024 77	0.012 08		0.000 24
p-Xylene	H^E	−472.797	−10.603	19.220		0.10
	V^E	−0.295 53	−0.017 34	0.005 87	−0.011 08	0.000 23

[a] Units: H^E, J mol^{-1}; V^E, cm^3 mol^{-1}.

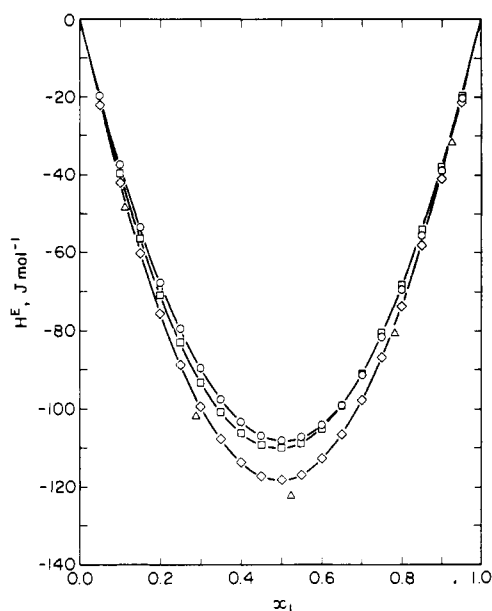**Figure 5.** Molar excess enthalpies of chlorobenzene (1)–isomeric xylene (2) at 298.15 K: o-xylene, O, present work; m-xylene, □, present work; p-xylene, ◊, present work; △, Harsted and Thomsen (7) at 293.15 K. Solid curves are least-squares representations of our results by eq 1.
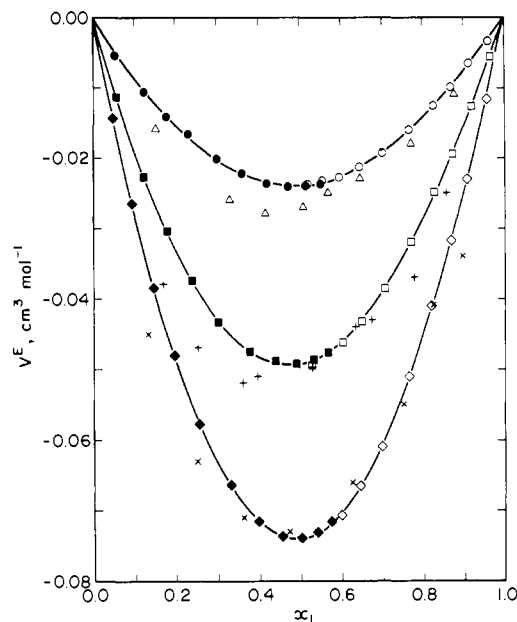

Figure 6. Molar excess volume of chlorobenzene (1)–isomeric xylene (2) at 298.15 K: o-xylene, O and ●, present work (two separate dilutions); △, Nigam et al. (11); m-xylene, □ and ■, present work (two separate dilutions); +, Nigam et al. (11); p-xylene. ◊ and ◆, present work (two separate dilutions); X, Nigam et al. (11). Solid curves are least-squares representations of our results by eq 1.

Note Added in Proof: Since the submission of this paper, excess enthalpies for chlorobenzene–isomeric xylene mixtures at 298.05 K have been published by R. K. Nigam, P. P. Singh, and N. N. Maini, *J. Chem. Thermodyn.*, **8**, 159 (1976). These have large deviations from our results.

Acknowledgment

We are indebted to P. J. D'Arcy and C. J. Halpin for technical assistance during this investigation.

Nomenclature

c_1, c_2, ... c_j = coefficients in representations of excess properties by eq 1
H^E = molar excess enthalpy, J mol^{-1}
m = number of experimental points in a set of results
n = number of coefficients in eq 1
n_D = refractive index for sodium light
V^E = molar excess volume, cm^3 mol^{-1}
X^E = typical molar excess property
x_i = mole fraction of component i

Greek Letters

σ = standard error defined in eq 2

Subscripts

1 = chlorobenzene
2 = aromatic hydrocarbon

Literature Cited

(1) American Petroleum Institute Research Project 44. Chemical Thermodynamics Properties Center, Texas A&M University, College Station, Texas. (See Table 5a dated Oct 31, 1950.)
(2) Becker, F., Schmahl, N. G., Pflug, H. D., *Z. Phys. Chem. (Frankfurt am Main)* **39**, 306 (1963).
(3) Bhattacharyya, S. N., Anantaraman, A. V., Palit, S. R., *Physica (Utrecht)*, **28**, 633 (1962).
(4) Canning, J., Cheesman, G. H., *J. Chem. Soc.*, 1230 (1955).
(5) Fenby, D. V., *Rev. Pure Appl. Chem.*, **22**, 55 (1972).
(6) Harris, K. R., Dunlop, P. J., *J. Chem. Thermodyn.*, **2**, 813 (1970).
(7) Harsted, B. S., Thomsen, E. S., *J. Chem. Thermodyn.*, **7**, 369 (1975).
(8) IUPAC Commission on Thermodynamics and Thermochemistry, *Bull. Thermodyn. Thermochem.*, **13**, 507 (1970).
(9) Letcher, T. M., Bayles, J. W., *J. Chem. Eng. Data*, **16**, 266 (1971).

(10) Murakami, S., Benson, G. C., J. Chem. Thermodyn., 1, 559 (1969).
(11) Nigam, R. K., Maini, N. N., Dhillon, M. S., Indian J. Chem., 11, 1288 (1973).
(12) Nigam, R. K., Singh, P. P., Trans. Faraday Soc., 65, 950 (1969).
(13) Nigam, R. K., Singh, P. P., Dhillon, M. S., Indian J. Chem., 7, 336 (1969).
(14) Nigam, R. K., Singh, P. P., Dhillon, M. S., Maini, N. N., Indian J. Chem., 8, 658 (1970).
(15) Nigam, R. K., Singh, P. P., Maini, N. N., Indian J. Chem., 8, 908 (1970).
(16) Recko, W. M., Sadowska, K. W., Bull. Acad. Pol. Sci., Ser. Sci. Chim, 17, 307 (1969).

(17) Riddick, J. A., Bunger, W. B., "Techniques of Chemistry", Vol. II, A. Weissberger, Ed., Wiley-Interscience, New York, N.Y., 1970.
(18) Tanaka, R., D'Arcy, P. J., Benson, G. C., Thermochim. Acta, 11, 163 (1975).
(19) Tanaka, R., Kiyohara, O., D'Arcy, P. J., Benson, G. C., Can. J. Chem., 53, 2262 (1975).
(20) Tanaka, R., Murakami, S., Fujishiro, R., J. Chem. Thermodyn., 6, 209 (1974).

Influence of Temperature on the Liquid–Liquid Equilibrium of the Water–n-Butyl Alcohol–Sodium Chloride System

R. De Santis,[†] L. Marrelli,* and P. N. Muscetta[‡]

Cattedra di Principi di Ingegneria Chimica, Facoltà di Ingegneria dell'Università di Roma, Italy

Experimental data are reported for the liquid–liquid equilibrium of the water–n-butyl alcohol–sodium chloride system in the range 20–40 °C. The observed Setschenow constants are compared with the results of the scaled-particle theory.

In a previous work (4) a thorough research was carried out on the liquid–liquid equilibria of ternary systems, water–sodium chloride–saturated aliphatic alcohol with three or four carbon atoms, at a temperature of 25 °C. The aim of the analysis was to characterize the thermodynamic behavior of these systems which have been extensively studied with respect to vapor–liquid equilibrium. In addition the interpretation of experimental results showed n-butyl alcohol (NBA) to be the most suitable of the series examined for sea water desalination by solvent extraction (2, 4, 13). However, NBA is inferior in selectivity to certain secondary and tertiary amines (3). The importance of the H_2O–NBA–NaCl system requires a more complete characterization of the temperature dependence of the salting-out effect. The only experimental results in literature seem to be those obtained by Reber et al. (17), concerning the NaCl effect on the mutual solubility of NBA and H_2O in the salt concentration range 0.02–0.08 (mole fractions) and for temperatures between 90 °C and the critical solubility temperature of the water–alcohol binary system.

Comparison of the observed Setschenow (19) constants with the values estimated by the scaled particle theory (10, 14, 15, 20) is also a matter of great interest.

Experimental Section

The measurements of the solubility limits have been carried out at 20, 30, and 40 °C using separator funnels with a thermostatic jacket for temperature control (±0.1 °C). Extractors were loaded with equal quantities of NBA and NaCl solution at concentrations between zero and the saturation value in the water. Experiments at 20 °C were carried out with three ratios (1, 1/3, 3 wt) of aqueous salt solution/alcohol. After an extended period of mixing and a quantitative gravity separation, samples were withdrawn from both phases. Equilibrium compositions were determined by analyzing the alcohol in the aqueous phase

† Istituto di Chimica Applicata e Metallurgia, Facoltà di Ingegneria dell'Università di Cagliari.
‡ Società Italiana Resine, Milano.

and the salt in both phases. Water and alcohol concentrations in the organic phase were derived from a material balance based upon the initial quantities and compositions.

The sodium chloride determinations were carried out with a Philips conductivitymeter. Alcohol in the aqueous phase was determined by colorimetric analysis (double beam Lange colorimeter) of the cerium complex, as proposed by Reid and Salmon (18). Each of the determinations was carried out with several repetitions. The standard deviations were derived and yielded reproducibilities in each case of 0.005 as weight fractions.

The alcohol used in the tests was obtained from Carlo Erba with analytical purity and was refractionated before use. Sodium chloride, RP purity, was obtained from Carlo Erba; dissolution water was prepared by a double distillation.

The experimental results on weight compositions of organic and aqueous phases for the different temperatures are shown in Tables I–III.

Discussion

The measurements of the solubility limits for the water–alcohol binary system at 20, 30, and 40 °C, and those at 25 °C (4), have been compared with data reported by other authors (1, 5, 6, 8). Figure 1 shows a good agreement between our observations and those reported in the literature.

The salt effect on the mutual water–alcohol solubility is shown in Figure 2. It is observed that salt induces a gradual miscibility gap which increases in width with the salt concentration.

Temperature effects, in the analyzed range, are similar to those observed for the binary system.

Temperature and salt concentration affect also the salt distribution between the two phases.

It can be observed (Figure 3), in this case, that the temperature effect is very small but such as to determine, as temperature increases, higher salt concentrations in the organic phase.

Salt concentration in the aqueous phase, instead, yields an increase of salt content in the organic phase. This effect becomes gradually smaller as salt concentration in the aqueous phase increases.

In addition Figure 4 represents the NBA distribution curves which show alcohol concentration in the organic phase increasing as temperature decreases.

Davison et al. (3) found that, with tertiary and secondary amines, the solvent free selectivity was a function only of the mole fraction of water in the solvent phase, being approximately